

Reduction of acute photodamage in skin by topical application of a novel PARP inhibitor

Beatrix Farkas^{a,*}, Marta Magyarlaki^a, Bela Csete^a, Jozsef Nemeth^b, Gyorgy Rabloczky^c, Sandor Bernath^c, Peter Literáti Nagy^c, Balazs Sümegi^d

^aDepartment of Dermatology, Faculty of Medicine, University of Pecs, Kodaly u. 20, H-7624 Pecs, Hungary

^bDepartment of Pharmacology, Faculty of Medicine, University of Pecs, Pecs, Hungary

^cN-Gene Research Laboratories Inc., Budapest, Hungary

^dDepartment of Biochemistry, Faculty of Medicine, University of Pecs, Pecs, Hungary

Received 14 May 2001; accepted 29 November 2001

Abstract

The ultraviolet (UV) components of sunlight induce damage to the DNA in skin cells, which is considered to be the initiating step in the harmful biological effects of UV radiation. Repair of DNA damage results in the formation of single-strand DNA breaks, which activate the nuclear poly(ADP-ribose) polymerase (PARP). Overactivation of PARP worsens the oxidative cell damage and impairs the energy metabolism, raising the possibility that moderation of PARP activation following DNA damage may protect skin cells from UV radiation. The topical effects of the novel PARP inhibitor *O*-(3-pyridino-2-hydroxy-1-propyl) pyridine-3-carboxylic acid amidoxime mono-hydrochloride (BGP-15M) were investigated on UV-induced skin damage in a hairless mouse model. For evaluation of the UV-induced acute photodamage to the skin and the potential protective effect of BGP-15M, DNA injury was detected by measuring the formation of single-strand DNA breaks and counting the resulting sunburn (apoptotic) cells. The ADP-ribosylation of PARP was assessed by Western blot analysis and then quantified. In addition, the UV-induced immunosuppression was investigated by the immunostaining of tumor necrosis factor alpha and interleukin-10 expressions in epidermal cells. The signs of inflammation were examined clinically and histochemically. Besides its primary effect in decreasing the activity of nuclear PARP, topically applied BGP-15M proved to be protective against solar and artificial UV radiation-induced acute skin damage. The DNA injury was decreased ($P < 0.01$). An inhibition of immunosuppression was observed by down-regulation of the epidermal production of cytokines IL-10 and TNF α . In the mouse skin, clinical or histological signs of UV-induced inflammation could not be observed. These data suggest that BGP-15M directly interferes with UV-induced cellular processes and modifies the activity of PARP. The effects provided by topical application of the new PARP-regulator BGP-15M indicate that it may be a novel type of agent in photoprotection of the skin. © 2002 Elsevier Science Inc. All rights reserved.

Keywords: Photodamage; PARP-inhibitor; Poly-ADP-ribosylation; DNA damage; Immunosuppression; Photoprotection

1. Introduction

The UV components of sunlight are now recognized as major environmental factors deleterious to human health

[1–4]. Skin cancer is the most common malignancy among Caucasians [2,4–7]. Photodamage, specific damage produced in the skin tissue by single or repeated (cumulative) exposure to UV light (290–400 nm), is considered to be the initiating step of photocarcinogenesis [8]. UV radiation-induced injury to the skin can be subdivided into acute (e.g. sunburn) and chronic (e.g. photoaging, solar keratosis and skin cancers) photodamage. At the molecular level, there is evidence that UV radiation generates DNA damage to skin cells either directly by producing cyclobutane pyrimidine dimer (CPD) and pyrimidine (6–4) pyrimidone photoproducts, or indirectly by increasing the level of reactive oxygen species (ROS), which facilitate DNA oxidation.

* Corresponding author. Tel.: +36-72535-815; fax: +36-72535-811.

E-mail address: farkasb@derma.pote.hu (B. Farkas).

Abbreviations: UV (A, B), ultraviolet (A, B); TNF α , tumor necrosis factor alpha; IL-10, interleukin-10; CPD, cyclobutane pyrimidine dimer; ROS, reactive oxygen species; ATP, adenine triphosphate; IgG, immunoglobulin G; MED, minimal erythema dose; H&E, hematoxylin and eosin; SCs, sunburn cells; F, fluorescence; D, percentage of double-stranded DNA; ECL, enhanced chemiluminescence; TBS, Tris buffered saline; AEC, aminoethylcarbazole; Th, T-helper; MHC, main histocompatibility complex.

These processes are involved in many biological effects of UV exposure, including photoaging, immunosuppression, photocarcinogenesis, etc. [9–11]. High doses of UV irradiation (sunlight) induce extensive DNA damage that impairs the DNA repair capacity, and results in permanent DNA damage which can be responsible for the deleterious effects of UV radiation [12,13]. These observations have led to the development of new strategies (e.g. liposome-encapsulated T4 endonuclease V, a bacterial DNA repair enzyme) to facilitate DNA repair in human cells and improve photoprotection [11]. The data suggest that other enzymes and molecules which decrease DNA damage and/or improve repair can be used as photoprotective agents.

It is well known that PARP (EC 2.4.2.30, 113 kDa), an evolutionarily conserved nuclear enzyme, is a constitutive factor of the DNA damage surveillance network developed by eukaryotic cells to cope with the numerous environmental and endogenous genotoxic agents [14]. Nuclear PARP is activated by single-strand DNA breaks when the enzyme is bound to broken ends of DNA, and is inactivated when released as a result of auto-ADP-ribosylation [15–17]. PARP uses NAD (β -nicotinamide adenine dinucleotide) as its substrate to synthesize poly-(ADP-ribose) and ADP ribosylates different nuclear proteins. Extensive DNA damage leads to excessive PARP activation, which induces the depletion of NAD⁺ and adenine triphosphate (ATP) finally resulting in cellular dysfunction and necrotic cell death [17–19]. It is now evident that PARP plays an essential role as a survival factor in replicating cells, which have suffered limited DNA damage. In contrast, extensive DNA damage seems to be directly related to the overactivation of PARP, to the disturbance of the energy balance of the cells, and to the manifestation of pathological processes (e.g. ischemia–reperfusion injury, diabetes, septic shock, etc.), which can be significantly ameliorated by genetic inactivation or pharmacological inhibition of PARP [14,17,20].

Previously, we observed the protective effect of *O*-(3-pyridino-2-hydroxy-1-propyl) pyridine-3-carboxylic acid amidoxime dihydrochloride (BGP-15), a new PARP-regulator, against ischemia–reperfusion-induced oxidative injury in a Langendorff-perfused heart model system. Our data suggested that BGP-15 moderated ischemia–reperfusion-induced oxidative damage, down-regulated the overactivation of PARP and improved the recovery of macroerg phosphates [21,22].

In this paper we studied the protective effect of BGP-15M against artificial and natural UV radiation-induced acute skin injuries. Using a hairless mouse model, we investigated the effects of BGP-15M on UV-induced DNA damage, PARP activation, sunburn cell formation and immunosuppression raising the possibility that down-regulation of PARP activity can produce photoprotection in the skin.

2. Materials and methods

2.1. Chemicals

Test preparations of BGP-15 and BGP-15M for dermal application, in a cream formulation (containing the active ingredient BGP-15M in 5, 10, 15 or 20%) as its vehicle, were obtained from N-Gene Research Laboratories Inc. poly(ADP-ribose)-specific monoclonal antibody was a kind gift from Alexander Buerkle (Heidelberg, Germany) and Masanao Miwa (Tsukuba, Japan). Interleukin-10 (IL-10)-specific serum (goat antimouse) and the antimouse immunoglobulin G (IgG) peroxidase complex were purchased from Sigma. Biotinylated antigoat antibody was from Jackson. The Immunotech Universal Kit was from Immunotech. Rabbit antimouse tumor necrosis factor alpha (TNF α) polyclonal antibody was obtained from Calbiochem, antirabbit IgG biotinylated species-specific whole donkey antibody was from Amersham, Vectastain Elite Kit and NovaRed Substrate Kit from Vector Co. were used. ¹⁴C-labeled BGP-15 (total activity: 17.9 MBq, specific activity: 443.6 MBq/g, radiochemical purity: 97.2%) was provided by the Institute for Drug Research Ltd. The Ultima-Gold liquid scintillation cocktail from Packard and the Protosol tissue solubilizer from NEN Products were used. All other reagents were of the highest purity commercially available.

2.2. Experimental animals

The experiments were carried out on hairless (VAF/plus CRL:hr/hr BR) mice (age: 6–8 weeks, weighing 21–25 g) purchased from Charles River Ltd. The animals were group-housed under pathogen-free conditions, with 12 hr light/dark periods a day, at a temperature of 22–25° and a humidity of 50–70%. They were provided with standard chow for mice and water *ad libitum*. Individual animals were identified by color painting of the ear. The cages were identified by identity cards. The experiments performed conformed to the European Community guiding principles for the care and use of laboratory animals. All animal care procedures and experimental protocols were approved by the Committee for the Care and Use of Laboratory Animals at the University of Pecs.

2.3. UV light source

A Waldmann UV 8001K light booth (Waldmann) equipped with UV21 Philips lamps (13 tubes) was used as UVB source. The major peak of these lamps is at 313 nm (within the UVB range). The irradiance was measured with a calibrated IL700 spectroradiometer with a cosine-corrected SEE 400 detector and a WBS 320 filter (International Light). The animals were placed at a distance of 30 cm from the lamps. In some experiments, solar exposure was used.

2.4. Phototesting of mouse skin

The minimal erythema dose (MED) energy of UV irradiation required to produce the minimally perceptible erythema reaction of the skin [23] was determined on six unprotected skin surface areas (0.25 cm^2) of animals exposed to increasing doses ($0.07\text{--}0.32 \text{ J/cm}^2$ with an increment of 0.05) of UVB. All other body sites were covered. Reading was carried out 24 hr after UV exposure by the same physician in order to avoid interobserver variations.

2.5. Treatment with BGP-15M cream or its vehicle

Test areas (1 cm^2 uncovered skin of mice) were treated either with BGP-15M cream or vehicle (2 mg cream/cm^2 of skin surface) 15 min prior to erythematogenic 2–4 MED UV exposure. Native skin (from untreated and unexposed animals) and BGP-15M cream-treated, but unexposed skin samples served as controls. The experiments were carried out under self-control circumstances. Tissue samples were collected either immediately (e.g. to determine ADP-ribosylation) or 24 hr after UV exposure. Skin samples were either snap-frozen at the optimal cold temperature and stored at -70° , or fixed in formalin.

2.6. Clinical investigation

Clinical examinations were carried out immediately and 24 hr after UV exposure. Signs of acute UV damage, erythema (e) and edema (ed) formation in unprotected skin areas were assessed visually, compared to the controls and evaluated by using the Draize score system, ranging from 0 to 4 (0: no e, 1: very slight e, 2: well defined e, 3: moderate e, 4: severe e; 0: no ed, 1: very slight ed (barely perceptible), 2: slight ed (edge of area displays a well defined raising), 3: moderate ed (raised approximately 1 mm), 4: severe ed (raised more than 1 mm) 24 hr after UV irradiation. A dermatoscope was used and photodocumentation was made.

2.7. Histological investigation

Tissue samples were fixed in 4% neutral-buffered formalin for undetermined lengths of time and were embedded in paraffin. The formalin-fixed, paraffin-embedded $4\text{--}6 \mu\text{m}$ tissue sections were deparaffinized, dehydrated in graded alcohol, and stained with hematoxylin and eosin (H&E) [24].

2.8. Detection of sunburn cells

Tissue samples were fixed in 4% buffered formalin, embedded in paraffin, sectioned at $4 \mu\text{m}$, and stained with H&E. The specimens were examined microscopically for sunburn cells (SCs) by the same observer. SCs (eosino-

philic cells with or without pyknotic nuclei) were counted at $400\times$ magnification in the interfollicular epidermis located above a 0.25 mm long part of the basement membrane (measured with a calibrated eyepiece micrometer), in 16 fields per animal and 80 fields per group. Counts were expressed as the mean number \pm SEM of SCs per mm length of epidermis.

2.9. Determination of skin absorption of BGP-15

The BGP-15 contents in the skin, serum and muscle of hairless mice were determined with ^{14}C -labeled BGP-15, used as an aqueous solution containing 30% of BGP-15. The animals were treated with a single topical application of a $4 \mu\text{L/cm}^2$ solution (radioactivity: 16,547,000 cpm per mouse) for 6 hr. The ^{14}C -labeled BGP-15-treated animals were divided into two groups. One group was exposed to 1 MED UVB light immediately after the topical application of the radioactive substance, while the animals in the other group were unexposed. An untreated-unexposed (native) group of mice served as controls. Each group contained five animals. At the end of the treatment (after 6 hr), the mice were anesthetized (100 mg ketamine/kg, i.p.) and killed. From animals, blood samples (1 mL per mouse) were collected; following centrifugation (10,000 rpm for 10 min, 4°), $50 \mu\text{L}$ serum was added to 5 mL liquid scintillation cocktail in a glass vial and the radioactivity of each serum sample was determined on a beta-counter (Beckman LS5000TD) for 5 min at room temperature. After measurement of the wet weight (20–40 mg), the collected skin and muscle samples were dissolved in 1 mL tissue solubilizer (48 hr, 60°) in glass scintillation vials. Following solubilization, the yellow samples were treated with $200 \mu\text{L} \text{ H}_2\text{O}_2$ (32% w/v) for 1 hr at room temperature, and finally 8 mL liquid scintillation cocktail was added to the colorless dissolved samples. The radioactivity of each sample was measured. The results were expressed as cpm/mL or cpm/g wet tissue.

2.10. Determination of single-strand DNA breaks

Single-strand DNA breaks were determined by the alkaline *F* analysis of DNA unwinding, as described by Birnboim and Jevcak [25]. DNA samples were prepared from the native (untreated and unexposed), 15% BGP-15M-containing cream-treated, 15% BGP-15M-containing cream or vehicle-pretreated and sun-exposed (4 MED UV) skin of mice. To estimate the quantity of undamaged double-stranded DNA, samples were divided into three sets of tubes. DNA *F* was determined under different conditions. To determine the *F* value, the DNA was kept at pH 12.4 to permit its partial unwinding. To determine F_{\min} , the DNA was kept at pH 12.4, but at the beginning of the incubation period the DNA sample was sonicated for 60 s. To determine F_{\max} , the DNA sample was kept at pH 11.0, which is below the pH needed to induce unwinding.

Solutions were incubated for 30 min at 0°, followed by a 15 min incubation at 15°. Unwinding was stopped by adjusting the pH to 11.0. Fluorescence was measured after addition of the dye (ethidium bromide, 0.67 µg/mL) at an excitation wavelength of 520 nm and an emission wavelength of 590 nm on a Perkin-Elmer luminescence spectrometer. Results are expressed as D (percentage of double-stranded DNA) = $(F - F_{\min})/(F_{\max} - F_{\min}) \times 100$.

2.11. ADP-ribosylation assay

The ADP-ribosylation of nuclear proteins was determined as described previously [21]. Briefly, skin samples (20 mg) were homogenized in 250 µL 50 mM Tris at pH 7.8 with an Ultra Turrax, 250 mL 2× Laemmli sample buffer containing 8 M urea was then added, and the mixtures were homogenized with a Potter-Elvehjem homogenizer, and cleared by centrifugation (5 min, 10,000 rpm). Samples were subjected to SDS-PAGE [26], using an 8% gel, and blotted to a nitrocellulose membrane for Western blot analysis. ADP-ribosylated proteins were detected with anti-poly(ADP-ribose) monoclonal antibody and the anti-mouse IgG peroxidase complex, and visualized by the enhanced chemiluminescence (ECL) method. Western blot signal intensities were quantitated with the ImageTool (Version 1.27) image processing program (University of Texas, Health Science Center, San Antonio).

2.12. Detection of ADP-ribosylation by immunohistochemical analysis

Six micro-meter tissue sections were cut in a cryostat, mounted on glass slides and fixed in cold acetone (4°, 10 min). Slides stained with H&E were reviewed to confirm the quality of tissue samples. Immunohistochemical staining was carried out with the anti-poly(ADP-ribose) monoclonal antibody (dilution of 1:1000 in Tris buffered saline (TBS), room temperature, 60 min) according to the streptavidin–biotin–peroxidase technique with H₂O₂/aminoethylcarbazole (AEC) development, using the Immunotech Universal Kit. Immunostaining with ascites fluid from non-immunized mice served as negative control [27].

2.13. Detection of UV-induced immunosuppression by immunostaining of TNFα and IL-10

UV-induced immunosuppression in mouse skin was determined via the TNFα and the IL-10 production by epidermal cells. Immunohistochemical staining of formalin-fixed paraffin-embedded tissue sections was carried out with anti-TNFα polyclonal antibody (dilution of 1:100 in TBS, room temperature, 60 min) or anti-IL-10 polyclonal antibody (dilution of 1:1000 in TBS, room temperature, 60 min) according to the streptavidin–biotin–peroxidase technique (with biotinylated antirabbit or antigoat antibody), using the Vectastain Elite Kit or Immunotech Universal Kit. Slides incubated with non-immune serum served as negative control [27].

2.14. Data analysis

Statistical analysis was performed by ANOVA and all of the data were expressed as means ± SEM. Student's *t*-test for unpaired comparison was used and *P* values <0.05 were considered to be significant. Each experimental group contained at least five animals.

3. Results

3.1. Effect of UV irradiation on dermal absorption of ¹⁴C-BGP-15

Radiolabeled-BGP-15 was used to provide information on the dermal absorption of BGP-15 and to study the potential influence of UVB radiation on the pharmacokinetic properties of the substance in the skin. In spite of the high dose BGP-15 administration (1200–1400 mg/kg body weight), the serum concentration of ¹⁴C-BGP-15 proved to be very low (0.00097% of the applied total radioactivity: 16,547,000 cpm per mouse (100%)), determined 6 hr after topical treatment. The mean net radioactivity of the serum in animals exposed to UV light was significantly lower (*P* < 0.01) than that observed in UV unexposed animals (Table 1). However, UV light exposure significantly (*P* < 0.01) increased the radioactivity of the skin as compared to

Table 1
Effects of UVB radiation on the dermal absorption of ¹⁴C-BGP-15 radioactivity in the skin

| Treatment | ¹⁴ C-BGP-15 radioactivity and BGP-15 content in | | | | | |
|------------------------------|--|--------------------|--------------------------|-----------------|--------------------------|----------------|
| | Serum | | Skin | | Muscle | |
| | Radioactivity (cpm/mL) | Content (ng/mL) | Radioactivity (cpm/g) | Content (ng/g) | Radioactivity (cpm/g) | Content (ng/g) |
| ¹⁴ C-BGP-15 | 844 ± 7.8 | 182 ± 1.7 | 1100000 ± 60000 | 240000 ± 10000 | 140000 ± 11000 | 31000 ± 2000 |
| ¹⁴ C-BGP-15 + UVB | 160 ± 9.6* | 35 ± 2.1* | 3280000 ± 130000* | 710000 ± 14000* | 180000 ± 20000 | 39000 ± 2000 |

The dermal absorption and pharmacokinetic properties of BGP-15 were investigated by using the radiolabeled substance. For details, see Section 2. Values are means ± SEM for 10 samples per group. Values different from ¹⁴C-BGP-15-treated values at a significance level of **P* < 0.001.

Table 2

Protective ability of BGP-15M against erythema, edema and sunburn cell formation in hairless mouse skin

| Treatment | Erythema mean score ± SEM | Edema mean score ± SEM | Sunburn cells/mm epidermis mean score ± SEM |
|-------------------------------|---------------------------|------------------------|---|
| Unexposed–untreated (control) | None | None | 0.5 ± 0.2 |
| Vehicle + UV | 2.8 ± 0.2 | 1.2 ± 0.3 | 37.4 ± 1.4 |
| 5% BGP-15M + UV | 0.7 ± 0.3** | 0.3 ± 0.2* | 8.8 ± 0.4* |
| ≥10% BGP-15M + UV | None | None | 1.6 ± 0.3** |

Clinical signs (erythema and edema) were evaluated with the Draize score system in vehicle- or BGP-15M-pretreated, UV exposed skin and compared with the untreated–unexposed native control. Sunburn cells were detected in H&E-stained specimens, using 80 fields per group. For details, see Section 2. Values are means ± SEM for six animals per group. Values different from vehicle-pretreated. UV exposed values at a significance level of **P* < 0.01. UV exposed values at a significance level of ***P* < 0.001.

that determined in UV unexposed animals. There was no significant difference (*P* > 0.05) in the contents of BGP-15 measured in muscle samples taken from UV exposed or unexposed animals (Table 1). On topical application, the radioactivity levels of ¹⁴C-BGP-15 and its metabolites determined in the sera were negligible. The data showed that topically applied ¹⁴C-BGP-15 was predominantly retained in the skin and UV light exposure further increased the skin content of BGP-15 in hairless mice.

3.2. BGP-15M cream pretreatment prevented the clinical and histological signs of sunburn in mouse skin

The photoprotective ability of BGP-15M cream (concentration: 5–20%) was tested in groups of hairless mice (six animals per group) exposed to a single erythematogenic 2 MED UVB radiation. Mice with untreated–unexposed (native control) and 20% BGP-15M cream-treated unexposed (irritancy-control) test areas served as controls. A single 2 MED UVB exposure produced an intense red discoloration (score for erythema: 3) with slight edema (score: 2) in the vehicle-pretreated skin areas of five of the six animals (Table 2). One animal exhibited well defined erythema (score: 2) without edema. In the group of mice pretreated with 5% BGP-15M cream prior to UV exposure, “well defined” erythema with “very slight” edema (scores: 2 and 1, respectively) were detected in one case, and a slight pink discoloration (score for erythema: 1) with very slight edema (score: 1) in the test areas in two animals. The skin in test areas of animals pretreated with ≥10% BGP-15M cream prior to UV exposure proved to be unchanged. The mean sum scores of the clinical signs are listed in Table 2. Under the given circumstances, the 10% BGP-15M cream furnished complete protection against acute UV damage to the skin. No signs of irritation were observed.

BGP-15M cream was tested at concentrations ≥10% for its effects on solar exposure (4 MED) in groups of animals (five mice per group). The 10% BGP-15M cream protected the skin from the establishment of the clinical and histological signs of sunburn (Figs. 1 and 2). In the test areas of mice pretreated with the vehicle and exposed to the Sun, lilac-red erythema with edema was observed 24 hr after exposure (Fig. 1). Histological examination revealed an

exulcerated epidermis with bandlike inflammatory infiltrates in the dermal connective tissue (Fig. 2C). Skin samples of mice pretreated with BGP-15M cream prior to UV exposure were histologically unaffected (Fig. 2B). The substance BGP-15M proved to be photoprotective. The photoprotective concentration of this novel PARP inhibitor on topical application was ≥10%.

3.3. BGP-15M cream reduced the number of sunburn cells in UV irradiated skin

The formation of sunburn cells (apoptotic keratinocytes) in the skin following UV irradiation is thought to be a

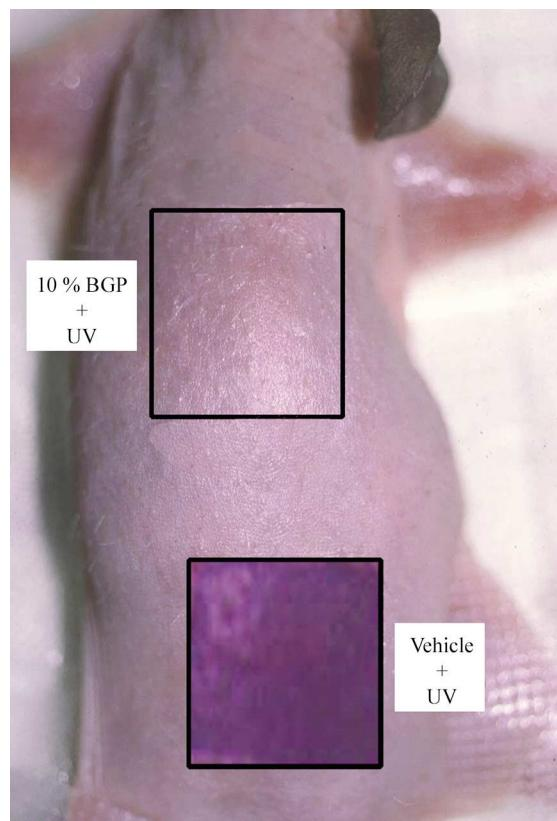


Fig. 1. Effects of BGP-15M cream on clinical signs of sunburn. The proximal skin surface area of the animal was pretreated with 10% BGP-15M cream, and the distal one with vehicle 15 min prior to solar exposure (4 MED UV). Clinical investigation was made 24 hr after solar exposure.

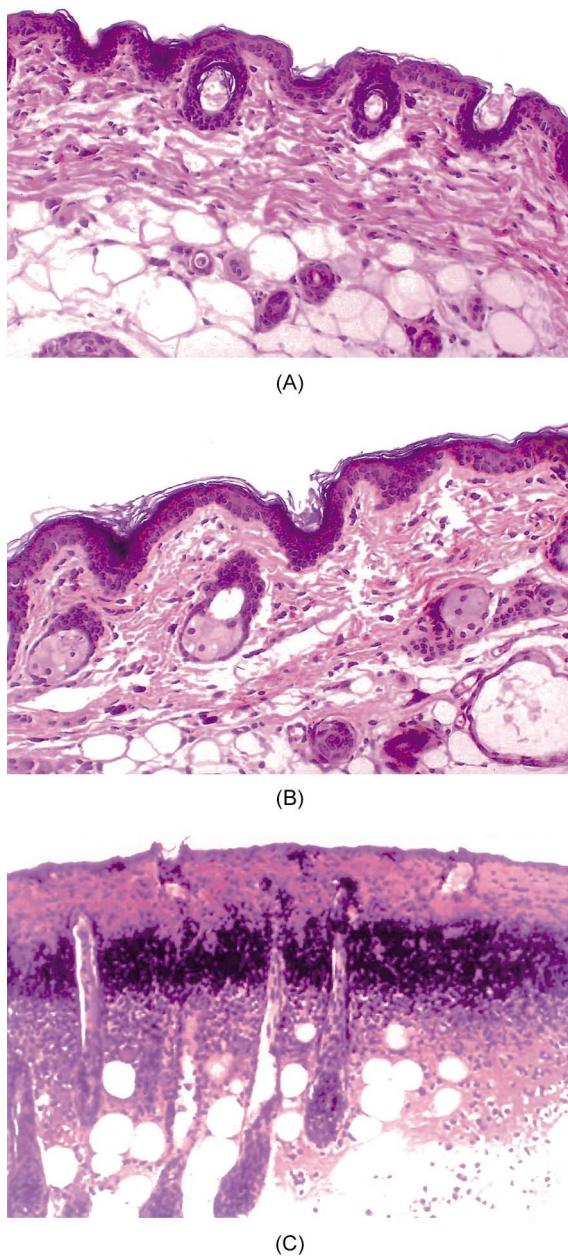


Fig. 2. Effect of BGP-15M cream on histological signs of sunburn. Histological samples derived from untreated–unexposed control skin (A), from 10% BGP-15M-pretreated, 4 MED UV exposed skin (B), and from vehicle-pretreated, UV exposed skin (C). Observations were made 24 hr after UV exposure (H&E, 200 \times).

consequence of UV-induced DNA damage [9]. Study of the DNA-protective ability of topically applied BGP-15M by the determination of SC-formation in H&E-stained specimens derived from vehicle- and BGP-15M cream-pretreated 2 MED UVB exposed skin samples, such as from native control skin revealed the following findings: in UVB exposed samples pretreated with $\geq 5\%$ BGP-15M cream, the mean number of SC formed was statistically significantly decreased ($P < 0.01$) as compared to the number observed in vehicle-pretreated samples (Table 2; Fig. 3). The reduced extent of formation of SCs in the BGP-

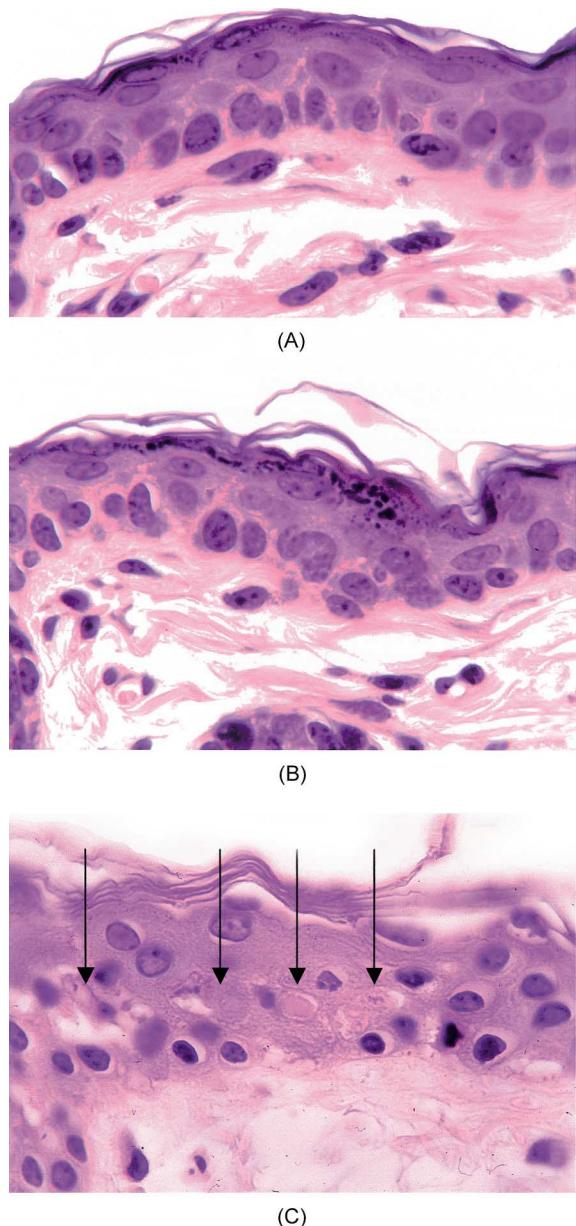


Fig. 3. BGP-15M cream reduced the number of sunburn cells in UV irradiated skin. Sunburn cells (apoptotic keratinocytes) were investigated in H&E-stained specimens derived from untreated–unexposed control (A), 10% BGP-15M cream-pretreated, 2 MED UVB exposed (B), and vehicle-pretreated, UV exposed (C) skin samples counted at 400 \times magnification in the interfollicular epidermis located above a 0.25 mm long part of the basement membrane. Formation of SCs, indicated by arrows, is revealed in vehicle-pretreated, UV exposed mouse skin (C) (H&E, 400 \times).

15M-pretreated UV exposed mouse skin confirms the photoprotective ability of this substance.

3.4. BGP-15M cream reduced single-strand DNA break formation in UV exposed skin

The high dose of UV radiation involved in exposure to sunlight generates DNA damage in the skin by producing pyrimidine dimers and increasing the level of ROS [28].

Table 3

Effects of BGP-15M on UV irradiation-induced single-strand DNA break formation in mouse skin

| Type of treatment | Non-damaged DNA (%) |
|-------------------------------|------------------------|
| Untreated-unexposed (control) | 80.7 ± 6 |
| 15% BGP-15M | 78.1 ± 7 |
| Vehicle + UV | 26.5 ± 4 ^{**} |
| 15% BGP-15M + UV | 52.4 ± 5 [*] |

Single-strand DNA breaks were determined by the alkali unwinding assay as described in Section 2. Values are means ± SEM for five skin preparations. Values different from the UV exposed, vehicle-pretreated values at a significance level of ${}^*P < 0.01$. Values different from the control values at a significance level of ${}^{**}P < 0.001$.

Under our experimental conditions, most of the DNA in unexposed-untreated (native) skin was undamaged, although UV exposure did induce a large amount of single-strand DNA breaks (undamaged DNA <30%) (Table 3). As shown in Table 3, BGP-15M pretreatment decreased the amount of single-strand breaks and significantly increased the quantity of undamaged DNA in the UV exposed skin. Topically applied BGP-15M provides protection by preventing the formation of DNA damage.

3.5. BGP-15M reduced ADP-ribosylation

Under the experimental conditions applied, the ADP-ribosylation level in the untreated-unexposed (native control) skin of the animals ($n = 5$) was hardly detectable, indicating that the number of DNA breaks (the signal for PARP activation) under these circumstances is extremely low (Table 4; Fig. 4). Although erythematogenic, 4 MED UV exposure induced an excessive activation of the self-ADP-ribosylation of PARP in the vehicle-pretreated skin of mice, as determined by Western blot analysis, pretreatment of the mouse skin with ≥10% BGP-15M-containing cream decreased the UV-induced ADP-ribosylation of PARP (Fig. 4). The quantitative analysis of Western blot signals demonstrated that topical treatment with BGP-15M at the applied concentrations resulted in more than 50% inhibition of the self-ADP-ribosylation of PARP (Table 4).

The immunohistological analysis of the epidermal cells from the vehicle-pretreated, UV exposed skin showed an intensive nuclear staining when anti-poly(ADP-ribose) antibody was used (Fig. 5B). In accordance with the results

Table 4

Effects of topically applied BGP-15M on the ADP-ribosylation of PARP in the skin

| Type of skin treatment | Signal intensity in arbitrary units ± SD |
|--|--|
| Untreated-unexposed (negative control) | 2 ± 1 |
| Vehicle-UV exposed | 51 ± 6 |
| 10% BGP-15M cream + UV | 23 ± 2 |
| Vehicle-UV exposed | 48 ± 4 |
| 20% BGP-15M cream + UV | 21 ± 3 |
| Vehicle-UV exposed | 47 ± 5 |
| PARP (positive control) | 52 ± 4 |

Western blot signal intensities were quantitated with IT-Tools image processing program. For details, see Section 2.

of Western blot analysis of the BGP-15M-pretreated samples, the number of epidermal cells with nuclear staining in the BGP-15M-pretreated UV exposed samples was reduced (Fig. 5A).

3.6. BGP-15M cream reduced the UVB exposure-induced production of TNF α and IL-10 in epidermal cells

Skin exposed to UVB radiation suppresses the induction of T cell-mediated responses, such as contact hypersensitivity and delayed-type hypersensitivity, by altering the function of the immune cells and causing the release of immunoregulatory cytokines (e.g. TNF α , IL-10, etc.) [29,30]. TNF α and IL-10 production in UV irradiated mouse skin was determined by immunohistological staining. A strong cytoplasmic and membrane TNF α expression could be observed in the UV exposed vehicle-pretreated epidermal cells 24 hr after UVB radiation of hairless mouse skin (Fig. 6C). Epidermal TNF α expression in skin samples taken from ≥10% BGP-15M-pretreated UV irradiated skin was not observed (Fig. 6B). The cytoplasmic staining for IL-10 in keratinocytes of the UV exposed vehicle-pretreated skin was intensive (Fig. 7C) comparing to the untreated-unexposed control (Fig. 7A). Only very rare cytoplasmic staining for IL-10 was observed among the epidermal cells in samples derived from ≥10% BGP-15M-pretreated UV irradiated skin (Fig. 7B). These mean that topically applied BGP-15M (≥10%) suppresses the UV-induced TNF α and IL-10 production of the epidermal cells, suggesting that BGP-15M treatment may prevent UV-induced immunosuppression in the mouse skin.

Western blot signal intensities of PARP

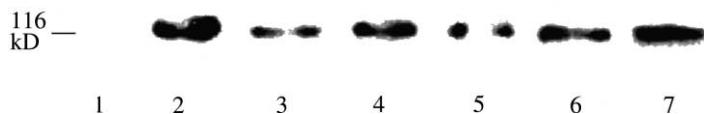
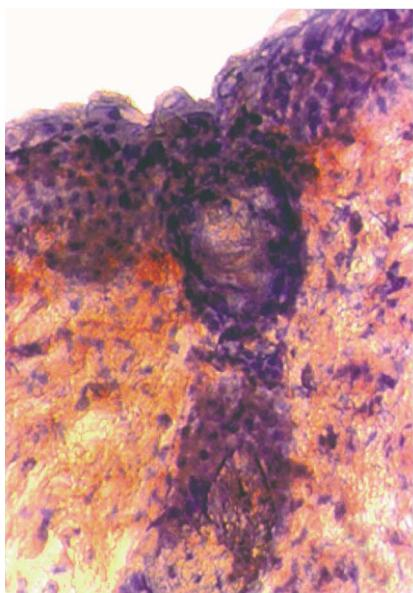
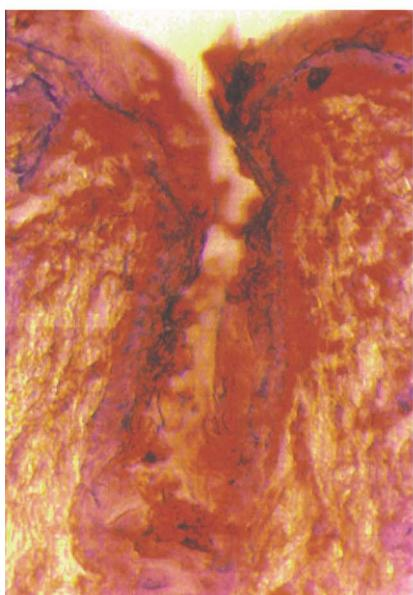


Fig. 4. ADP-ribosylation of PARP, determined by Western blot analyses. ADP-ribosylation of PARP was studied in skin specimens taken immediately after erythematogenic UV exposure, using Western blot analyses. For details, see Section 2. ADP-ribosylation levels of unexposed-untreated (native) skin (lane 1), UV irradiated, vehicle-pretreated mouse skin (lanes 2, 4 and 6), 10% BGP-15M-pretreated (lane 3) or 20% BGP-15M-pretreated (lane 5), UV exposed skin. ADP-ribosylated PARP was used as a positive control (lane 7).



(A)

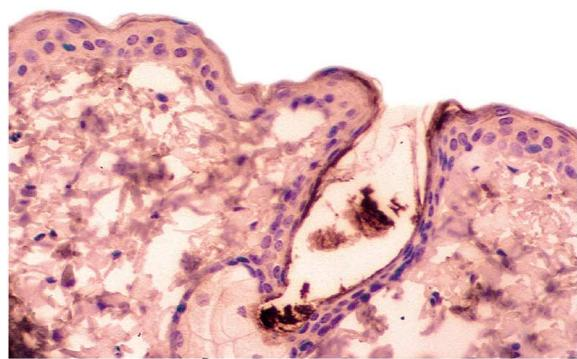


(B)

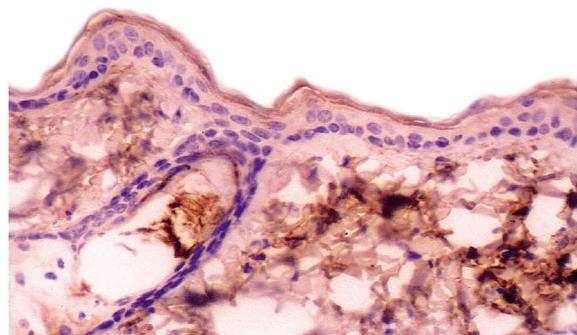
Fig. 5. ADP-ribosylation of PARP determined by immunochemical staining. ADP-ribosylation of PARP was studied in skin specimens taken 30 min after erythematogenic UV exposure. Immunohistochemical staining of frozen tissue sections was carried out with anti-poly(ADP-ribose)-specific monoclonal antibody. For details, see Section 2; 20% BGP-15M-pretreated, UV irradiated skin (A), and UV exposed, vehicle-pretreated skin (B). The immunostaining of connective tissue and inflammatory cells is non-specific (result of a cross-reactivity of a second antisera on murine tissue) (magnification: 400 \times).

4. Discussion

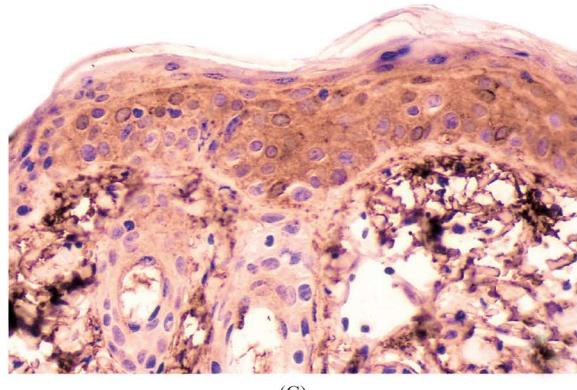
The UV rays of sunlight penetrate into the skin as a function of their wavelengths. Radiation of shorter wavelengths (UVB, 290–320 nm) is mostly absorbed in the epidermis and interacts predominantly with keratinocytes. Radiation of longer wavelengths (UVA, 320–400 nm)



(A)



(B)



(C)

Fig. 6. TNF α staining of epidermal cells in UV exposed skin. UV-induced immunosuppression in mouse skin was determined by the production of TNF α in epidermal cells. Immunohistochemical staining of formalin-fixed, paraffin-embedded tissue sections was carried out with anti-TNF α polyclonal antibody. For details, see Section 2. Untreated-unexposed control (A), 15% BGP-15M-pretreated, UV irradiated skin (B), and UV exposed, vehicle-pretreated skin (C) (magnification: 400 \times).

penetrates deeper, affecting the epidermal and dermal cells. Convolution of the spectra with biological damage action spectra shows that, despite the significantly greater incidence of UVA radiation (95% of the UV reaching the Earth), the predominant acute and chronic damages to the skin are associated with the UVB portion of the solar spectrum [31–33].

The skin is vulnerable to the ROS produced by photochemical reactions with UV light and ionizing radiation [34,35]. The ROS are involved in various pathological conditions of the skin (e.g. inflammation, phototoxic

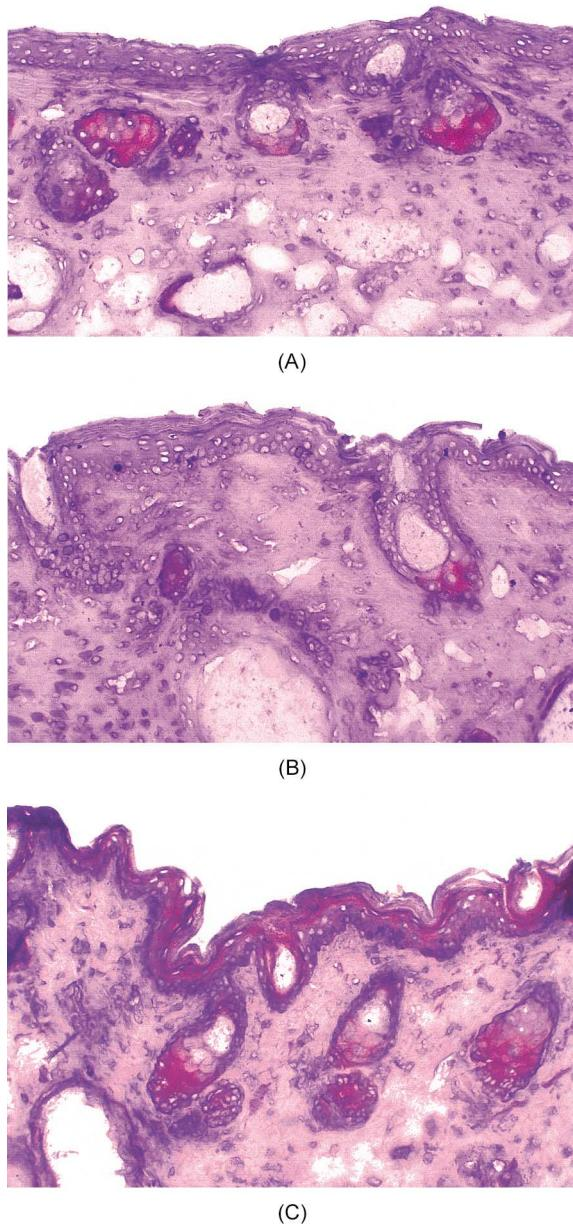


Fig. 7. IL-10 staining of epidermal keratinocytes in UV exposed skin. UV-induced immunosuppression in mouse skin was examined via the IL-10 protein expression by the epidermal keratinocytes. Immunohistochemical staining of formalin-fixed, paraffin-embedded tissue sections was carried out with anti-IL-10 polyclonal antibody. For details, see Section 2. Untreated-unexposed control (A), 10% BGP-15M-pretreated, UV irradiated skin (B), and UV exposed, vehicle-pretreated skin (C) (magnification: 200 \times).

reactions, photoaging, photocarcinogenesis, etc.) [28,35–37]. Cellular DNA has been considered to be the principle molecular target for most of the biological effects of UV radiation [1,38,39]. It has been shown that UVA rays mostly act indirectly, by generating ROS which can subsequently exert a multitude of effects, such as lipid peroxidation, activation of transcription factors and generation of DNA strand breaks [40]. While UVB light can also generate ROS, it is most effective in direct interaction with DNA, with the formation of DNA photo-

products (thymine dimers), which are converted into single-strand DNA breaks via DNA repair enzymes [2,3,28,41,42]. The acute effects of UV light such as sunburn and the role of UV radiation in immunosuppression and in the induction of non-melanoma skin cancers (squamous and basal cell carcinomas) developed from keratinocytes, are overwhelmingly attributed to UVB portion of the solar spectrum [31,33]. It can be assumed, therefore, that the exposure of mouse skin to UV radiation may induce the formation of a detectable amount of single-strand DNA breaks, which, in turn, activate PARP. Excessive PARP activation (very rapid synthesis and degradation of poly(ADP-ribose) chains) may exhaust the energy pools, and are characterized by rapid cell injury [43–46].

It is well known that PARP inhibitors protect different types of cells against ROS-induced injury, but little information is available on the role of PARP inhibitors in UV-induced photodamage to the skin [47–50]. We therefore designed experiments to investigate the potential protective function of a novel non-toxic PARP-regulator, BGP-15M, in the mechanism of action involving epidermal cells in UV radiation (solar or artificial)-induced skin injury.

To provide information on the dermal absorption of BGP-15 and the influence of UV radiation on the pharmacokinetic properties of the substance in mouse skin, a ^{14}C -BGP-15 solution was used. ^{14}C -BGP-15 applied topically is predominantly retained in the skin. Furthermore, UV light exposure promoted the accumulation of BGP-15 in the skin (Table 1). Systemic side-effects of the substance proved to be negligible (Table 1).

In skin samples exposed to erythematogenic (4 MED) UV radiation, the poly-ADP-ribosylation of PARP was intensive, which is likely the consequence of the excessive DNA break formation. This process could be significantly reduced by using BGP-15M topically in a concentration of $\geq 10\%$ (Table 4; Fig. 4). This finding was in agreement with our previous observations that *in vitro* BGP-15 inhibited isolated PARP with $\text{IC}_{50} = 120 \mu\text{M}$ at 1 mM NAD $^+$ in Langendorff-perfused hearts [21].

PARP activation is generally considered to be a consequence of the oxidative cell damage mediated by single-strand DNA break formation [15,19]. Under our experimental conditions, UV radiation induced a large amount of single-strand breaks in the vehicle-pretreated hairless mouse skin, which could be decreased by topical treatment with BGP-15M prior to UV exposure (Table 3). There are data suggesting that PARP inhibitors partially protect mitochondrial respiration from externally added oxidant, but these inhibitors failed to protect the genome from single-strand DNA breaks [51,52]. Contrary to these observations BGP-15M significantly decreased the amount of DNA breaks in mouse skin (Table 3). It is likely that the ROS are generated predominantly by mitochondrial respiration and the protection of respiratory complexes by PARP inhibitors (regulators) can decrease the UV-induced mitochondrial ROS production [21,53]. However, it is also

possible that BGP-15M treatment by entrapping hydroxyl radicals (BGP-15 in 0.1–5 mM concentration range shows significant reactivity with hydroxyl radicals formed in Fenton reaction (unpublished data)) decreases oxidative cell damage and therefore lowers the amount of single-strand DNA breaks in epidermal cells.

There are observations suggesting that disruption of PARP gene makes mice more sensitive to DNA damage induced by nitrosamines than PARP^{+/+} mice, inspite of the fact that PARP^{-/-} mice develop normally without signs of genetic defects [54]. Our model is quite different from the PARP^{-/-} systems, since BGP-15M in the applied concentration is appropriate to suppress the UV radiation-induced overactivation of PARP but actual PARP activity still remains significantly higher than that in UV unexposed (native) control skin (Table 4). Therefore, the present results support studies showing that the down-regulation of excessive overactivation of PARP prevent the NAD⁺ and ATP depletion and necrotic cell death without compromising the DNA repair [47,55–60].

Since a correlation exists between the UV dose delivered and the formation of sunburn cells in the epidermis, the increase in the number of these apoptotic cells was simply regarded as a marker of the severity of solar damage [9,61–63]. Different molecular pathways (e.g. activation of tumor suppressor gene *p53*, triggering of cell death receptors either directly by UV or by autocrine release of death ligands, mitochondrial damage and cytochrome *c* release, etc.) and their interplay are thought to be involved in the UV-mediated apoptosis of keratinocytes [9,64–67]. It is known that the formation of sunburn cells is linked to the severity of UV-induced DNA damage [9]. Therefore, the observation that BGP-15M treatment significantly reduced the number of sunburn cells in UV exposed skin to that found in native (control) epidermis (Table 2; Fig. 3), supports the DNA-protective effect of BGP-15M applied topically.

UV radiation-induced ROS formation activates inflammatory reactions in the skin and contributes to the development of immunosuppression as a promoter of photocarcinogenesis [29,68–70]. Recent studies have demonstrated that the immunosuppressive and inflammatory reactions following UV radiation are regulated by the modulation of cytokines (e.g. IL-10, TNF α , IL-6, IL-1, IL-12) production of epidermal cells [71–75]. The up-regulation of TNF α and IL-10 induced by UVB radiation is known to have a central role in skin immunosuppression [73,74,76,77]. A correlation has been found between the restoration of immunity and the reduction in the levels of these cytokines [78,79]. TNF α and IL-10 production by the epidermal cells was therefore utilized to test the effects of BGP-15M on UV-induced immunosuppression. BGP-15M pretreatment prior to solar exposure reduced the level of TNF α and IL-10 in the mouse epidermis close to the control value (Figs. 6 and 7), suggesting that BGP-15M treatment prevents UV-induced immunosuppression in the skin.

The data suggest that BGP-15M, directly interfering with UV-induced cellular processes and modifying the activity of PARP, may be a novel type of skin protective agent against UV-induced photodamage.

Acknowledgments

We are grateful to Gy. Szekeres for the histochemistry of IL-10. We thank Csilla Juhász, B. Horvath and L. Girán for their excellent technical help. This work was supported by grants from N-Gene Research Laboratories Inc., from the Hungarian Science Foundation T034320, from the Ministry of Health and Welfare ETT 35/2000.

References

- [1] Freeman SE, Hacham H, Gange RW, Maytum DJ, Sutherland JC, Sutherland BM. Wavelength dependence of pyrimidine dimer formation in DNA of human skin irradiated *in situ* with ultraviolet light. Proc Natl Acad Sci USA 1989;86:5605–9.
- [2] Katiyar SK, Matsui MS, Mukhtar H. Kinetics of UV light-induced cyclobutane pyrimidine dimers in human skin *in vivo*: an immuno-histochemical analysis of both epidermis and dermis. Photochem Photobiol 2000;72:788–93.
- [3] Berton TR, Mitchell DL, Fischer SM, Locniskar MF. Epidermal proliferation but not the quantity of DNA photodamage is correlated with UV-induced mouse skin carcinogenesis. J Invest Dermatol 1997;109:340–7.
- [4] Bykov VJ, Marcusson JA, Hemminki K. Protective effects of tanning on cutaneous DNA damage *in situ*. Dermatology 2001;202:22–6.
- [5] Kraemer KH. Sunlight and skin cancer: another link revealed. Proc Natl Acad Sci USA 1997;94:11–4.
- [6] Bykov VJ, Sheehan JM, Hemminki K, Young AR. *In situ* repair of cyclobutane pyrimidine dimers and 6–4 photoproducts in human skin exposed to solar simulating radiation. J Invest Dermatol 1999;112:326–31.
- [7] Marrot L, Belaïdi JP, Chaubo C, Meunier JR, Perez P, Agapakis-Causse C. An *in vitro* strategy to evaluate the phototoxicity. Eur J Dermatol 1998;8:403–12.
- [8] Gilchrest BA. A review of skin ageing and its medical therapy. Br J Dermatol 1996;135:867–75.
- [9] Kulms D, Schwarz T. Molecular mechanisms of UV-induced apoptosis. Photodermatol Photoimmunol Photomed 2000;16:195–201.
- [10] Sailstad DM, Boykin EH, Slade R, Doerfler DL, Selgrade MJK. The effect of a Vitamin A acetate diet on ultraviolet radiation-induced immune suppression as measured by contact hypersensitivity in mice. Photochem Photobiol 2000;72:766–71.
- [11] Yarosh D, Klein J, O'Connor A, Hawk J, Rafal E, Wolf P. Effect of topically applied T4 endonuclease V in liposomes on skin cancer in xeroderma pigmentosum: a randomised study. Lancet 2001;357:926–9.
- [12] Wolf P, Maier H, Mullegger RR, Chadwick CA, Hofmann-Wellenhof R, Soyer HP, Hofer A, Smolle J, Horn M, Cerroni L, Yarosh D, Klein J, Bucana C, Dunner Jr. K, Potten CS, Höningmann H, Kerl H, Kripke ML. Topical treatment with liposomes containing T4 endonuclease V protects human skin *in vivo* from ultraviolet-induced up-regulation of interleukin-10 and tumor necrosis factor alpha. J Invest Dermatol 2000;114:149–56.
- [13] Wei Q, Matanoski GM, Farmer ER, Hedayati MA, Grossman L. DNA repair capacity for ultraviolet light-induced damage is reduced

- in peripheral lymphocytes from patients with basal cell carcinoma. *J Invest Dermatol* 1995;104:933–6.
- [14] Shall S, de Murcia G. Poly(ADP-ribose) polymerase-1: what have we learned from the deficient mouse model? *Mutat Res* 2000;460:1–15.
- [15] Lindahl T, Satoh MS, Poirier GG, Klungland A. Post-translational modification of poly(ADP-ribose) polymerase induced by DNA strand breaks. *Trends Biochem Sci* 1995;20:405–11.
- [16] Smulson ME, Pang D, Jung M, Dimtchev A, Chasovskikh S, Spoonde A, Simbulan-Rosenthal C, Rosenthal D, Yakovlev A, Dritschilo A. Irreversible binding of poly(ADP-ribose) polymerase cleavage product to DNA ends revealed by atomic force microscopy: possible role in apoptosis. *Cancer Res* 1998;58:3495–8.
- [17] Niedergang C, Oliver JF, Menissier-de Murcia J, de Murcia G. Involvement of poly(ADP-ribose) polymerase in the cellular response to DNA damage. In: Szabó, C, editor. *Cell death: the role of poly(ADP-ribose) polymerase*. Boca Raton, FL: CRC Press, 1999. p. 183–207.
- [18] Radson J, Heller B, Burkle A, Hartmann B, Rodriguez ML, Kroncke KD, Burkart V, Kolb H. Nitric oxide toxicity in islet cells involves poly(ADP-ribose) polymerase activation and concomitant NAD depletion. *Biochem Biophys Res Commun* 1994;199:1270–1.
- [19] Szabó C, Zingarelli B, O'Connor M, Salzman AL. DNA strand breakage, activation of poly(ADP-ribose) synthetase, and energy depletion are involved in the cytotoxicity of macrophages and smooth muscle cells exposed to peroxynitrite. *Proc Natl Acad Sci USA* 1996;93:1753–8.
- [20] Zhang J, Li J-H. Poly(ADP-ribose) polymerase inhibition by genetic and pharmacological means. In: Szabó, C, editor. *Cell death: the role of poly(ADP-ribose) polymerase*. Boca Raton, FL: CRC Press, 1999. p. 279–305.
- [21] Szabadoss E, Literáti-Nagy P, Farkas B, Sümegei B. BGP-15, a nicotinic amidoxime derivative protecting heart from ischemia-reperfusion injury through modulation of poly(ADP-ribose) polymerase. *Biochem Pharmacol* 2000;59:937–45.
- [22] Halmosi R, Berente Z, Ósz E, Tóth K, Literáti-Nagy P, Sümegei B. Effect of poly(ADP-ribose) polymerase inhibitors on the ischemia-reperfusion-induced oxidative cell damage and mitochondrial metabolism in Langendorff heart perfusion system. *Mol Pharmacol* 2001;59:1497–505.
- [23] Lowe NJ, Friedlander J. Sunscreens: rationale for use to reduce photodamage and phototoxicity. In: Lowe NJ, Shaath NA, Pathak MA, editors. *Sunscreens*. New York: Marcel Dekker, 1997. p. 37–8.
- [24] Hould R. *Techniques d'histopathologie et de cytopathologie*. Paris: Maloine Éditeur, 1993.
- [25] Birnboim HC, Jevcak JJ. Fluorimetric method for rapid detection of DNA strand breaks in human white blood cells produced by low doses of radiation. *Cancer Res* 1981;41:1889–92.
- [26] Sümegei B, Melegh B, Adamovich K, Trombitas K. Cytochrome oxidase deficiency affecting the structure of the myofibre and the shape of mitochondrial cristae membrane. *Clin Chim Acta* 1990;192:9–18.
- [27] Mikel UV. Advanced laboratory methods in histology and pathology. Washington, DC: Armed Forces Institute of Pathology and Armed Registry of Pathology, 1994.
- [28] Krutmann J. The role of UVA rays in skin aging. *Eur J Dermatol* 2001;11:170–1.
- [29] Cruz JR, Leverkus PDM, Dougherty I, Gleason MJ, Eller M, Yaar M, Gilchrest BA. Thymidine dinucleotides inhibit contact hypersensitivity and activate the gene for tumor necrosis factor α . *J Invest Dermatol* 2000;114:253–8.
- [30] Fiorentino DF, Zlotnik A, Viera P, Mosmann TR, Howard M, Moore KW, O'Garra A. IL-10 acts on the antigen-presenting cell to inhibit cytokine production by Th1 cells. *J Immunol* 1991;146:3444–51.
- [31] Elmets CA, Singh D, Tubesing K, Matsui M, Katiyar S, Mukhtar H. Cutaneous photoprotection from ultraviolet injury by green tea polyphenols. *J Am Acad Dermatol* 2001;44:425–32.
- [32] Cole C. Sunscreen protection in the ultraviolet A region: how to measure the effectiveness. *Photodermat Photoimmun Photomed* 2001;17:2–10.
- [33] Lim HW, Naylor M, Höngsmann H, Gilchrest BA, Cooper K, Morison W, DeLeo VA, Scherschun L. American Academy of Dermatology Consensus Conference on UVA protection of sunscreens: summary and recommendations. *J Am Acad Dermatol* 2001;44:505–8.
- [34] Shallreuter KU, Wood JM. Free radical reduction in the human epidermis. *Free Radic Biol Med* 1989;6:519–32.
- [35] Maccarrone M, Catani MV, Iraci S, Melino G, Agro AF. A survey of reactive oxygen species and their role in dermatology. *J Eur Acad Dermatol Venereol* 1997;8:185–202.
- [36] Berneburg M, Grether-Beck S, Kürten V, Ruzicka T, Briviba K, Sies H, Krutmann J. Singlet oxygen mediates the UVA-induced generation of the photoaging-associated mitochondrial common deletions. *J Biol Chem* 1999;274:15345–9.
- [37] Steenvoorden DPT, Beijersbergen GMJ. The use of endogenous antioxidants to improve photoprotection. *J Photochem Photobiol B: Biol* 1997;41:1–10.
- [38] Hemminki K, Xu G, Le Curieux F. Ultraviolet radiation-induced photoproducts in human skin DNA as biomarkers of damage and its repair. *IARC Sci Publ* 2001;154:69–79.
- [39] Marrot L, Belaïdi JP, Chaubé C, Meunier JR, Perez P, Agapakis-Causse C. An *in vitro* strategy to evaluate the phototoxicity. *Eur J Dermatol* 1998;8:403–12.
- [40] Krutmann J, Croteau DL, Bohr VA. Repair of oxidative damage to nuclear and mitochondrial DNA in mammalian cells. *J Biol Chem* 1997;272:25409–12.
- [41] Green WB, McGuire PG, Miska KB, Kusewitt DF. Urokinase activity in corneal fibroblasts may be modulated by DNA damage and secreted proteins. *Photochem Photobiol* 2001;73:318–23.
- [42] Mitchell DL, Byrom M, Chiarello S, Lowery MG. Effects of chronic exposure to ultraviolet B radiation on DNA repair in the dermis and epidermis of the hairless mouse. *J Invest Dermatol* 2001;116:209–15.
- [43] D'Amours D, Desnoyers S, D'Silva I, Poirier GG. Poly-ADP-ribosylation reactions in the regulation of nuclear functions. *Biochem J* 1999;342:249–68.
- [44] Simbulan-Rosenthal CM, Rosenthal DS, Smulson ME. Pleiotropic roles of poly-ADP-ribosylation of DNA-binding proteins. In: Szabó C, editor. *Cell death: the role of poly(ADP-ribose) polymerase*. Boca Raton, FL: CRC Press, 1999. p. 252–3.
- [45] Abdelkarim GE, Gertz K, Harms C, Katchanov J, Dirnagl U, Szabó C, Endres M. Protective effects of PJ34, a novel potent inhibitor of poly(ADP-ribose) polymerase (PARP) in *in vitro* and *in vivo* models of stroke. *Int J Mol Med* 2001;7:255–60.
- [46] Szabadoss E, Fischer GM, Gallyas Jr. F, Kispál G, Sümegei B. Enhanced ADP-ribosylation and its diminution by lipoamide after ischemia-reperfusion in perfused rat heart. *Free Radic Biol Med* 1999;27:1103–13.
- [47] Szabó C, Virág L, Cuzzocrea S, Scott G, Hake P, O'Connor M, Zingarelli B, Salzman A, Kun E. Protection against peroxynitrite-induced fibroblast injury and arthritis development by inhibition of poly(ADP-ribose) synthase. *Proc Natl Acad Sci USA* 1998;95:3867–72.
- [48] Said SI, Berisha HI, Pakbaz H. Excitotoxicity in the lung: N-methyl-D-aspartate-induced, nitric oxide-dependent, pulmonary edema is attenuated by vasoactive intestinal peptide and by inhibitors of poly(ADP-ribose) polymerase. *Proc Natl Acad Sci USA* 1996;93:4688–92.
- [49] Endres M, Scott GS, Salzman AL, Kuhn E, Moskowitz MA, Szabó C. Protective effects of 5-iodo-6-amino-1,2-benzopyrone and inhibitor of poly(ADP-ribose) synthetase against peroxynitrite-induced glial damage and stroke development. *Eur J Pharmacol* 1998;351:377–82.
- [50] Cleaver JE, Bodell WJ, Borek C, Morgan WF, Schwartz JL. Poly(ADP-ribose): spectator or participant in excision repair of DNA damage. *Princess Takamatsu Symp* 1983;13:195–207.

- [51] Virág L, Salzman AL, Szabó C. Poly(ADP-ribose) synthetase activation mediates mitochondrial injury during oxidant-induced cell death. *J Immunol* 1998;161:3753–9.
- [52] Zingarelli B, Cuzzocrea S, Zsengeler Z, Salzman AL, Szabó C. Protection against myocardial ischemia and reperfusion injury by 3-aminobenzoid, an inhibitor of poly(ADP-ribose) synthetase. *Cardiovasc Res* 1997;36:205–15.
- [53] Vanden Hoek TL, Becker LB, Shao Z, Li C, Schumacker PT. Reactive oxygen species released from mitochondria during brief hypoxia induce preconditioning in cardiomyocytes. *J Biol Chem* 1998;273:18092–8.
- [54] Tsutsumi M, Masutani M, Nozaki T, Kusuoka O, Tsujiuchi T, Nakagama H, Suzuki H, Konishi Y, Sugimura T. Increased susceptibility of poly(ADP-ribose) polymerase-1 knockout mice to nitrosamine carcinogenicity. *Carcinogenesis* 2001;22:1–3.
- [55] Wang ZQ, Auer B, Stingl L, Berghammer H, Haidacher D, Schweiger M, Wagner EF. Mice lacking ADPRT and poly-ADP-ribosylation develop normally but are susceptible to skin disease. *Genes Dev* 1995;9:509–20.
- [56] de Murcia MJ, Niedergang C, Trucco C, Ricoul M, Dutrillaux B, Mark M, Oliver FJ, Masson M, Dierich A, LeMeur M, Walztinger C, Champon P, de Murcia G. Requirement of poly(ADP-ribose) polymerase in recovery from DNA damage in mice and in cells. *Proc Natl Acad Sci USA* 1997;94:7303–7.
- [57] Eliasson MJL, Sampei K, Mandir AS, Hurn PD, Traystman RJ, Bao J, Pieper A, Wang ZQ, Dawson TM, Snyder SH, Dawson VL. Poly(ADP-ribose) polymerase gene disruption renders mice resistant to cerebral ischaemia. *Nat Med* 1994;3:1089–95.
- [58] Mandir AS, Przedborski S, Jackson-Lewis V, Wang ZQ, Simbulan-Rosenthal D, Smulson ME, Hoffman BE, Guastella DB, Dawson VL, Dawson TM. Poly(ADP-ribose) polymerase activation mediates 1-methyl-4-phenyl-1,2,3,6-tetrahydropyridine (MPTP)-induced parkinsonism. *Proc Natl Acad Sci USA* 1999;96:5774–9.
- [59] Pieper A, Brat D, Krug D, Watkins CC, Gupta S, Blackshaw S, Verma A, Wang ZQ, Snyder S. Poly(ADP-ribose) polymerase-deficient mice are protected from streptozotocine-induced diabetes. *Proc Natl Acad Sci USA* 1999;96:3059–64.
- [60] Simbulan-Rosenthal CM, Haddad BR, Rosenthal DS, Weaver Z, Coleman A, Luo RB, Young HM, Wang ZQ, Ried T, Smulson ME. Chromosomal aberrations in PARP^{-/-} mice: genome stabilization in immortalized cells by reintroduction of poly(ADP-ribose) polymerase cDNA. *PNAS* 1999;96:13191–6.
- [61] Danno K, Horio T. Sunburn cell: factors involved in its formation. *Photochem Photobiol* 1987;45:683–90.
- [62] Kohen JJ. Apoptosis. *Immunol Today* 1993;14:126–30.
- [63] Woodcock A, Magnus IA. The sunburn cell in mouse skin. Preliminary quantitative studies on its production. *Br J Dermatol* 1976;95:459–68.
- [64] Kulms D, Pöppelmann B, Yarosh D, Luger TA, Krutmann J, Schwarz T. Nuclear and cell membrane effects contribute independently to the induction of apoptosis in human cells exposed to UVB radiation. *Proc Natl Acad Sci USA* 1999;96:7974–9.
- [65] Goldstein JC, Waterhouse NJ, Juin P, Evan GI, Green DR. The coordinate release of cytochrome *c* during apoptosis is rapid complete and kinetically invariant. *Nat Cell Biol* 2000;2:156–62.
- [66] Reed JC. Double identity for proteins of the Bcl-2 family. *Nature* 1997;387:773–6.
- [67] Pourzand C, Tyrrell RM. Apoptosis: the role of oxidative stress and example of solar UV radiation. *Photochem Photobiol* 1999;70:380–90.
- [68] Kripke ML, Cox PA, Alas LG, Jarosh DB. Pyrimidine dimers in DNA initiate systemic immunosuppression in UV irradiated mice. *Proc Natl Acad Sci USA* 1992;89:7516–20.
- [69] Horio T, Okamoto H. Oxygen intermediates are involved in ultraviolet radiation-induced damage of Langerhans cells. *J Invest Dermatol* 1987;88:699–702.
- [70] Moison RMW, Steenvorden DPT, Beijersbergen van Henegouwen GMJ. Topically applied eicosapentaenoic acid protects against local immunosuppression induced by UVB irradiation, *cis*-urocanic acid and thymidine dinucleotides. *Photochem Photobiol* 2001;73:64–70.
- [71] Shreedhar V, Giess T, Sung VW, Ullrich SE. A cytokine cascade including prostaglandin E2, IL-4, and IL-10 is responsible for UV-induced systemic immune suppression. *J Immunol* 1998;160:3783–9.
- [72] Enk AH, Katz SI. Identification and induction of keratinocyte-derived IL-10. *J Immunol* 1992;149:92–5.
- [73] Rivas JM, Ullrich SE. Systemic suppression of delayed-type hypersensitivity by supernatants from UV irradiated keratinocytes. *J Immunol* 1992;149:3865–71.
- [74] Skov L, Hansen H, Allen M, Villadsen L, Norval M, Barker JNWN, Simon J, Baadsgaard O. Contrasting effects of ultraviolet A1 and ultraviolet B exposure on the induction of tumour necrosis factor α in human skin. *Br J Dermatol* 1998;138:216–20.
- [75] Nishigori C, Yarosh DB, Ulrich SE, Vink AA, Bucana CD, Roza L, Kripke ML. Evidence that DNA damage triggers IL-10 cytokine production in UV irradiated murine keratinocytes. *Proc Natl Acad Sci USA* 1996;93:10354–9.
- [76] Zak-Prelich M, Norval M, Venner TJ, Bisset Y, Walker C, Rafferty TS, Sauder DN, McKenzie RC. *Cis*-urocanic acid does not induce the expression of immunosuppressive cytokines in murine keratinocytes. *Photochem Photobiol* 2001;73:238–44.
- [77] Monique H, Hurks H, Van der Molen RG, Out-Luiting C, Vermeer B-J, Mommaas AM. Differential effects of sunscreens on UVB-induced immunomodulation in humans. *J Invest Dermatol* 1997;109:699–703.
- [78] Byeon SW, Pelley RP, Ullrich SE, Waller TA, Bucana CD, Strickland FM. Aloe Barbadensis extracts reduce the production of interleukin-10 after exposure to ultraviolet radiation. *J Invest Dermatol* 1998;110:811–7.
- [79] Clingen PH, Berneburg M, Petit-Frère C, Woollons A, Lowe JE, Arlett CF, Green MHL. Contrasting effects of an ultraviolet B and ultraviolet A tanning lamp on interleukin-6, tumour necrosis factor α and intercellular adhesion molecule-1 expression. *Br J Dermatol* 2001;145:54–62.